Alpha-particle spectroscopic strengths in ^{19}F and ^{20}Ne

Z. Q. Mao, H. T. Fortune, and A. G. Lacaze
Department of Physics and Astronomy, University of Pennsylvania, Philadelphia, Pennsylvania 19104
(Received 7 August 1995)

We have measured angular distributions for the ^{15}N(^{6}Li,d)^{19}F and ^{16}O(^{6}Li,d)^{20}Ne reactions at a bombarding energy of 22 MeV. Distorted-wave Born approximation and Hauser-Feshbach calculations were used to analyze the data. Alpha spectroscopic factors were obtained for all the states up to 4.1 MeV in ^{19}F and 6 MeV in ^{20}Ne.

PACS number(s): 25.70.Hi, 21.10.Jx, 27.20.+n, 27.30.+t

I. INTRODUCTION

Alpha transfer reactions are useful in studying the alpha cluster structure of nuclei. At bombarding energies near 22 MeV, investigations of (^{6}Li,d) experiments in the mass region of $A=10$–20 have demonstrated that a direct reaction mechanism dominates [1,2]. In the laboratory energy range 19.8 and 32 MeV, House and Kemper [3] present excitation functions for ^{16}O(^{6} Li,d) for the ground state at an angle of 7.5°, for the 4.25-MeV 4^+ state at 17.5°, and for the 1.63-MeV 2^+ state at both angles. They made additional back-angles (155° and 165°) measurements at 20, 24, and 28 MeV. They report $\sigma(\text{forward})/\sigma(\text{backward})\sim 5-10$, $5-10$, and 3 for 0^+, 2^+, and 4^+, respectively, prompting them to conclude ''that statistical compound nuclear contributions are small in this reaction.'' (Of course, that conclusion is limited to the three states mentioned.) At a laboratory energy of 32 MeV Gunn *et al.* [4] present data for the same reaction, but leading to the low-lying negative-parity levels. They performed compound-nucleus (CN) and coupled-channels (CC) calculations. For the 2^- state, calculated CN and CC cross sections were comparable at angles of $30°-70°$, but CN dominated at forward ($0°-20°$) and backward ($\geqslant 110°$) angles. Because CN cross sections decrease dramatically as bombarding energy is increasing, their results imply that at our energy, population of the 2^- state will be dominated by CN.

For direct (^{6}Li,d) reactions, one can obtain alpha spectroscopic factors through distorted-wave Born approximation (DWBA) analysis. The alpha spectroscopic factors of ^{19}Ne have attracted attention because the resonance at 504 keV ($E_x=4033$ keV, $J^\pi=3/2^+$) above the ^{15}O+α threshold of 3529 keV in ^{19}Ne is important for the breakout of the hot CNO cycle in many astrophysical sites, such as nova and x-ray bursts [5]. Because ^{15}O is a radioactive nucleus, no direct measurement of the spectroscopic factor has been performed. However, the nuclei ^{19}F and ^{19}Ne are mirrors. Instead of measuring the alpha spectroscopic factors of ^{19}Ne, we could measure those for the mirror states in ^{19}F because they are the same.

To obtain experimental alpha-particle spectroscopic factors, we have measured the ^{15}N(^{6}Li,d)^{19}F and ^{16}O(^{6}Li,d)^{20}Ne reactions at a bombarding energy of 22 MeV. Distorted-wave Born approximation and Hauser-Feshbach (HF) calculations were performed in order to obtain the alpha spectroscopic factors for all the low-lying states.

The alpha decay width of an unbound state can also be obtained from the expression $\Gamma_\alpha = S_\alpha \Gamma_{\text{sp}}$, where Γ_{sp} is the alpha single-particle width and S_α is the alpha-stripping spectroscopic factor of the state. The single-particle width of a resonance can be calculated using the code ABACUS [6], approximating the alpha-nucleus potential by a real Woods-Saxon well. Details of such calculations are given later in the present paper.

II. EXPERIMENTAL PROCEDURES AND RESULTS

The experiment was performed with 22-MeV ^{6}Li^{+++} ions from the University of Pennsylvania tandem accelerator. Outgoing deuterons were momentum analyzed in a multi-angle spectrograph and detected on 25 μm NTA nuclear emulsion plates. Absorbers 0.03 cm in thickness, placed directly in front of the focal planes, prevented particles with $Z>1$ from reaching the emulsions. The ^{15}N target was gas in a closed cell containing isotopically enriched ^{15}N (99.5%). The gas cell had a 295 μg/cm^2 Mylar window. Indirect monitoring of the cell pressure was achieved by observing elastically scattered ^{6}Li in a Si surface barrier detector mounted at a lab angle of 30°. Deuteron spectra were recorded in 7.5° angular intervals, beginning at 7.5° and ending at 80.0°. A spectrum at 7.5° is presented in Fig. 1 for the

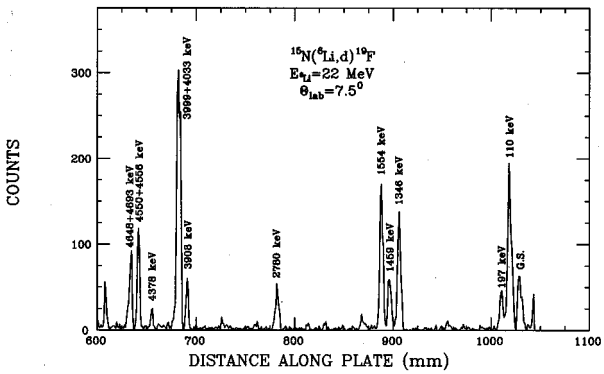

FIG. 1. Spectrum of the ^{15}N(^{6}Li,d)^{19}F reaction at a bombarding energy of 22 MeV and a laboratory angle of 7.5°. Peaks are labeled with their excitation energies from this work. Excitation energies and their standard deviations are listed in Table I.

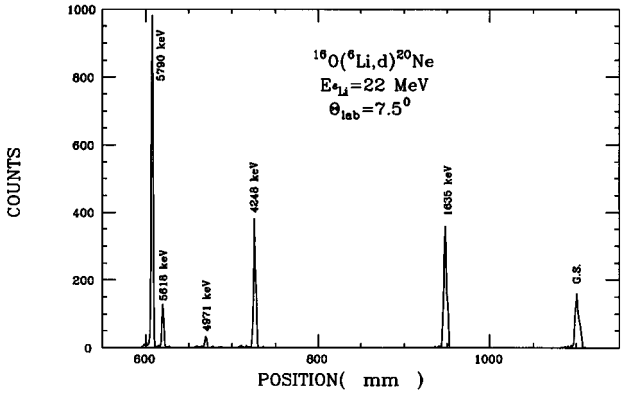

FIG. 2. Same as Fig. 1, but for the ^{16}O(^{6}Li,d)^{20}Ne reaction.

states below 4.7 MeV.

For the purpose of normalizing theoretical cross sections as outlined below, the ^{16}O(^{6}Li,d) angular distributions were also measured, using a natural oxygen gas target (99.8% of ^{16}O), at the same bombarding energy. For the purpose of normalizing HF cross sections, we did the measurement up to a laboratory angle 130°, which corresponds to a center-of-mass angle of about 135°. Figure 2 contains a spectrum for this reaction at 7.5°. Table I lists the present excitation energies for these states, in both ^{19}F and ^{20}Ne, in comparison to the listed values in [7].

Absolute cross sections were calculated using known cell geometry, gas pressure and integrated beam current. Relative uncertainties were taken to be the larger of 5% or the statistical uncertainty. The absolute scale of the cross sections is probably accurate to ±3%. Experimental angular distributions for states up to E_x=4.1 MeV are presented in Fig. 3. Figure 4 displays ^{20}Ne angular distributions up to 6 MeV.

TABLE I. Results from ^{15}N(^{6}Li,d) and ^{16}O(^{6}Li,d) in comparison with previous information.

Compilation [a]		Present work		
E_x (keV)	J^π	E_x (keV)	σ_{max} (mb/sr)	L
[^{19}F]				
0	$1/2^+$	2±3	0.055	1
110	$1/2^-$	117±3	0.15	0
197	$5/2^+$	198±3	0.050	3
1346	$5/2^-$	1347±3	0.18	2
1459	$3/2^-$	1458±3	0.12	2
1554	$3/2^+$	1558±3	0.13	1
2780	$9/2^+$	2781±3	0.040	5
3908	$3/2^+$	3906±3	0.016	1
3999	$7/2^-$	(4024±10)[b]	<0.20	4
4033	$9/2^-$	(4024±10)[b]	<0.20	4
[^{20}Ne]				
0	0^+	−2±3	0.15	0
1634	2^+	1635±3	0.23	2
4248	4^+	4248±3	0.17	4
4967	2^-	4971±3	0.015	1,3
5621	3^-	5618±3	0.050	3
5788	1^-	5790±3	0.31	1

[a]From [7].
[b]Unresolved.

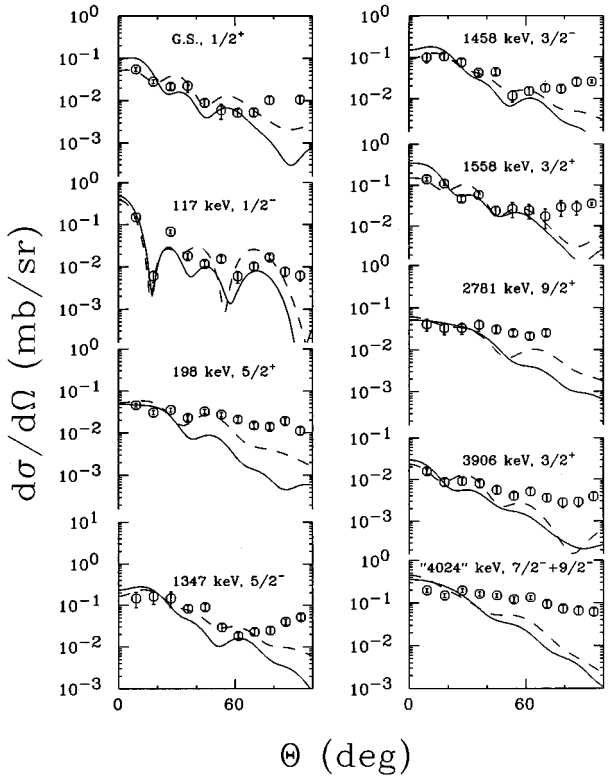

FIG. 3. Angular distributions of the ^{15}N(^{6}Li,d)^{19}F reaction for the states below 4.1 MeV. The curves are the theoretical results from the DWBA calculation using alpha radius of 1.94 fm (solid) and 1.40 fm (dashed). The theoretical cross sections were normalized to the experimental cross sections for each state, respectively.

III. ANALYSES

We have assumed the states of interest in the present study are populated through a pure one-step direct reaction mechanism in the DWBA calculation. In order to test the stability of the calculations, we have tried a few different optical potentials. For ^{6}Li, the 240-MeV potential used by Watson [8], the 190-MeV potential used by Strohbosch *et al.* [9] and Garrett *et al.* [10], the 159-MeV potential used by Garrett *et al.* [10], the 35.5-MeV potential (PL potential) used by Fortune *et al.* [11], and for the deuteron, the 105.0-MeV potential (PL potential) used by Fortune *et al.* [11] were chosen to test the DWBA calculations. The PL optical potentials (also see Table II) of Ref. [11] produced smooth behavior of the maximum differential cross sections when we varied the radius parameter and principal quantum numbers of the transferred alpha, for both the ^{15}N(^{6}Li,d) and ^{16}O(^{6}Li,d) reactions. The 1^- state in ^{20}Ne was used to obtain the N value in Eq. 1 (below).

The relationship between experimental and DWBA cross sections for α-stripping reactions is

$$\sigma_{\text{expt}} = NS_\alpha \frac{2J_f+1}{(2J_i+1)(2L+1)} \sigma_{\text{DW}}, \qquad (1)$$

where J_i and J_f are the spins of the target and residual nuclei, respectively, L is the angular momentum of the trans-

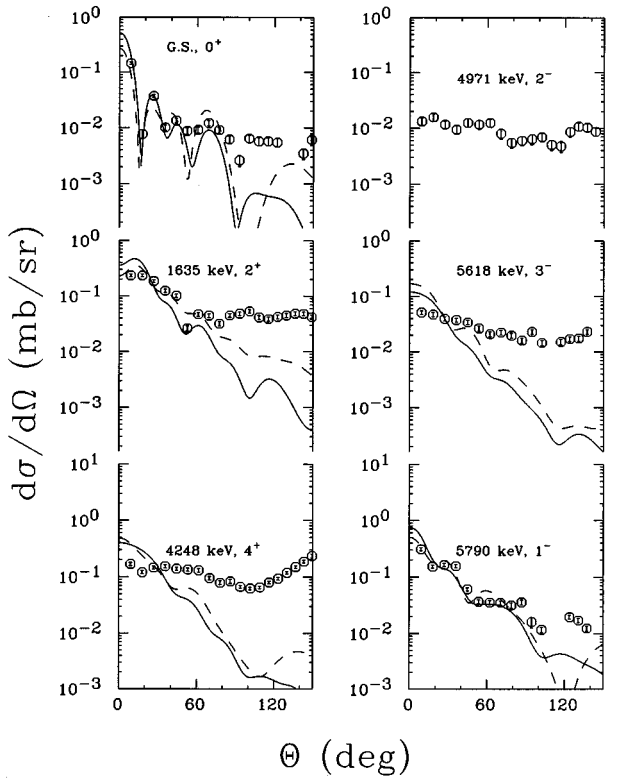

FIG. 4. Same as Fig. 3, but for the states below 6 MeV in ^{20}Ne from the ^{16}O(^{6}Li,d) reaction.

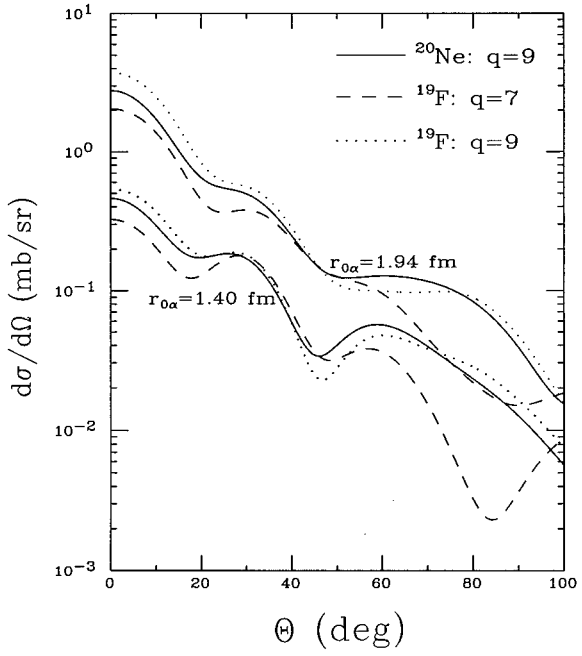

FIG. 5. Curves of DWBA cross sections of (^{6}Li,d) reactions for populating the 5.788-MeV, 1^- state in ^{20}Ne and the 3.908-MeV, $3/2^+$ state in ^{19}F, with different $(q, r_{0\alpha})$ pairs.

ferred alpha particle, S_α is the alpha spectroscopic factor, N is a constant related to the structure of the incident particle, and $\sigma_{\rm DW}$ is the cross section calculated using the code DWUCK4 [12]. For (^{6}Li,d) reactions, the value of N has to be determined experimentally because it is unknown theoretically. From Eq. (1), the value of N can be determined from comparing the DWBA cross section to the experimental cross section for a state if the alpha spectroscopic factor of it is known. For this purpose, we calculated the alpha spectroscopic factor of the first 1^- state (E_x=5788 keV) in ^{20}Ne from the comparison between its well-known alpha-particle width (Γ_α) and the alpha single-particle width ($\Gamma_{\rm sp}$), calculated by using the code ABACUS [6] ($S_\alpha=\Gamma_\alpha/\Gamma_{\rm sp}$). Then, the value of N can be determined by requiring that the S_α thus obtained causes the DWBA cross section to fit the experimental angular distribution of the 1^- state. Another advantage of choosing the ^{16}O(^{6}Li,d)^{20}Ne reaction is that ^{15}N (or ^{19}F) and ^{16}O (or ^{20}Ne) are similar in mass. This is important because optical potential parameters can be mass dependent.

In the calculation of the alpha single-particle width of the 5788 keV, 1^- state in ^{20}Ne, two alpha radii, 1.94 and 1.40 fm, respectively, were used. Values obtained were $\Gamma_{\rm sp}$=110 eV for r_0=1.94 fm and 31.2 eV for r_0=1.40 fm. Comparing to the experimental alpha decay width of 28±3 eV [7], the alpha spectroscopic factors for this state are 0.255 and 0.90, respectively.

We have performed DWBA calculations for two different values of the radius parameter of the alpha-particle potential well, viz., $r_{0\alpha}$=1.40 and 1.94 fm. We have used both q=7 and 9 for the total number of quanta of excitation. The latter is appropriate for $(sd)^3(fp)$ transfer, the former for $(1p)(sd)^3$. The 1^- state in ^{20}Ne is commonly thought to have q=9, and, in fact, to have a nearly pure SU3 configuration $(\lambda\mu)=(90)$. Curves of DWBA for these various possibilities are plotted in Fig. 5. We have also computed, with the code ABACUS [6], the α single-particle widths for ^{19}Ne ($3/2^+$) and ^{20}Ne (1^-) with the above values of $r_{0\alpha}$ and q. Table III summarizes the various DWBA cross sections at 9° and single-particle widths.

Using Eq. (1), the value of N=1.06 was obtained when the SET1 parameters ($r_{0\alpha}$=1.94 fm) were used, and 1.18 when the SET2 parameters ($r_{0\alpha}$=1.40 fm) were used. The value of N is relatively insensitive to changes in $r_{0\alpha}$ because $\sigma_{\rm DW}$ and $\Gamma_{\rm sp}$ both change when $r_{0\alpha}$ is varied. Thus S_α can be quite different, but N much less so.

TABLE II. Potential parameters used in the DWBA and alpha single-particle width calculations. (Strengths are in MeV, lengths in fm.)

Channel	V	$W'=4W_D$	r_0	a	r_0'	a'	r_{0c}
^{6}Li*	35.5	50.0	1.42	0.92	1.71	0.89	1.42
d[a]	105.0	98.0	1.02	0.86	1.42	0.65	1.02
α(SET1)	varied	...	1.94	0.60	...	...	1.94
α(SET2)	varied	...	1.40	0.60	...	...	1.40

[a]From [11].

TABLE III. DWBA cross sections of the 3.908-MeV, $3/2^+$ state in ^{19}F and 5.788-MeV, 1^- state in ^{20}Ne from the (^{6}Li,d) reactions at 9°, and α single-particle widths for the 4.033-MeV, $3/2^+$ in ^{19}Ne and the 5.788-MeV, 1^- state in ^{20}Ne.

$(q,r_{0\alpha})$	$(d\sigma/d\Omega)_{9°}(^{19}\mathrm{F})$	Γ_{sp} (eV)	$(d\sigma/d\Omega)_{9°}(^{20}\mathrm{Ne})$	Γ_{sp} (eV)
(9,1.40 fm)	0.398	1.99×10^{-4}	0.319	31.2
(9,1.94 fm)	2.71	1.09×10^{-3}	1.88	110
(7,1.40 fm)	0.223	1.39×10^{-4}		
(7,1.94 fm)	1.49	7.34×10^{-4}		

Shown in Fig. 4 are the DWBA angular distributions compared with the experimental ones in ^{20}Ne from the ^{16}O(^{6}Li,d) reaction. The same parameters used in this calculation were adopted for the ^{15}N(^{6}Li,d) reaction.

Because the one-step DWBA cross sections are smaller than the experimental cross section at backward angles, a two-step direct reaction mechanism or compound reaction mechanism could make contributions to the reaction, especially for weakly populated states. The experimental angular distribution (Fig. 4) of the first 2^- state of ^{20}Ne at an excitation energy of 4967 keV, populated in the ^{16}O(^{6}Li,d)^{20}Ne reaction, is observed to be approximately symmetric about 90°, thus indicating that this 2^- state is probably populated via a compound reaction mechanism. The compound reaction cross section for the 2^- state is about 10^{-2} mb/sr, which is about the same as those at large angles for most of the states in ^{19}F. Therefore, for (^{6}Li,d) reactions, a compound reaction mechanism is probably more likely than two-step processes. The code STATIS [13] calculates compound reaction cross sections by adopting the Hauser-Feshbach method. Because of the selection rule forbidding one-step direct reaction, and weak two-step process mechanisms in alpha transfer reaction, we analyzed the data for this 2^- state by assuming a pure compound reaction mechanism. Shown in Fig. 6 is the theoretical HF angular distribution in comparison with the experimental data. In addition to the incident ^{6}Li and exit d channels, the HF calculations included the four other channels which have the largest total compound reaction cross sections. These are ^{18}F+α, ^{21}Ne+p, ^{21}Na+n, and ^{19}F+^{3}He. A normalization factor of 0.61 was obtained from fitting the angular distribution of the 2^- state in ^{20}Ne. Inclusion of the HF contribution to ^{20}Ne (5788 keV, 1^-) reduces the N previously determined by less than 4%; hence we use the above N values throughout.

In the HF analysis of the ^{15}N(^{6}Li,d) reaction, for the same reason as for the ^{16}O(^{6}Li,d) reaction, six outgoing channels were considered. They are ^{15}N+^{6}Li, ^{19}F+d, ^{17}O+α, ^{20}F+p, ^{20}Ne+n, and ^{13}C+^{8}Be. The same normalization factor of 0.61 for compound reaction cross sections was applied in the comparison with experimental data.

The experimental angular distributions for the ten observed states in ^{19}F are shown in Fig. 3 along with DWBA curves obtained with the PL optical potential parameters (Table II). Solid curves in Fig. 3 were calculated using SET1 parameters for the alpha particle (Table II), where the potential radius for the transferred alpha particle is 1.94 fm. The angular distributions calculated with this radius parameter equals to 1.40 fm (SET2 parameters in Table II), are dashed in Fig. 3. In each fit, the normalizations of the theoretical curves were adjusted to fit the absolute experimental cross sections, resulting in alpha-particle spectroscopic factors listed in Table IV. Both sets of alpha parameters give reasonable fits to the angular distributions at forward angles. At backward angles, the DWBA cross sections are smaller than the experimental data, a fact which may hint that other reaction mechanisms contribute to the reaction when the cross section is small.

Figure 7 displays the angular distributions of the same 10 states, together with compound reaction cross sections from the HF calculation, direct reaction cross sections from the DWBA calculations, and their sum, using $r_{0\alpha}=1.94$ fm. Shown in Fig. 8 are the same as those in Fig. 7, but with $r_{0\alpha}=1.40$ fm. Incoherent sums of the DWBA and HF cross

TABLE IV. Alpha spectroscopic factors of the states in ^{19}F.

E_x [a] (keV)	J^π [a]	S_α(DWBA) [b]		S_α(DWBA+HF) [b]	
		1.94 (fm)	1.40 (fm)	1.94 (fm)	1.40 (fm)
0	$1/2^+$	0.13	0.74	0.11	0.66
110	$1/2^-$	0.15	1.1	0.13	1.1
197	$5/2^+$	0.031	0.34	0.025	0.28
1346	$5/2^-$	0.10	0.71	0.086	0.64
1459	$3/2^-$	0.091	0.55	0.085	0.53
1554	$3/2^+$	0.21	0.83	0.20	0.79
2780	$9/2^+$	0.015	0.17	0.010	0.12
3908	$3/2^+$	0.022	0.090	0.017	0.076
3999+4033	$7/2^-+9/2^-$	0.028	0.21	0.026	0.19

[a]From Ref. [7].

[b]The 5788-keV, 1^- state in ^{20}Ne was used as a normalization.

sections were used because the direct reaction and compound reaction have very different interaction time scale. A better agreement between the sum cross sections and the experimental data has been obtained at backward angles for the relatively weakly populated states [$(d\sigma/d\Omega) \leq 0.01$ mb/sr at backward angles]. For the $3/2^+$ state at 3908 keV, the sum cross section fits the data very well. However, the improvement is negligible for most of the strongly populated states. The HF cross sections are much smaller than the experimental cross sections at forward angles, indicating that the reaction was dominated by a direct reaction for the strong states.

The comparison between the theoretical results and the experimental data for ^{20}Ne states are shown in Figs. 6 and 9. For the DWBA curves in Fig. 6, the alpha radius used is 1.94 fm, but it is 1.40 fm in the calculation of Fig. 9. The compound contribution to the cross section of the 1^- state in ^{20}Ne can be ignored, even at backward angles.

Four different sets of alpha spectroscopic factors are obtained and listed from columns 3–6 in Tables IV and V for ^{19}F and ^{20}Ne, respectively. The uncertainties for the alpha spectroscopic factors were obtained from the fitting of the angular distributions. Therefore, they are relative. The absolute uncertainties might be larger. The differences of S'_α's between the DWBA alone and DWBA with HF are about 20% or less. However, the S'_α's for all the states are about a factor 4 larger for $r_\alpha = 1.40$ fm than those for $r_\alpha = 1.94$ fm.

The low-lying negative-parity states in ^{19}F, $1/2^-$ at $E_x = 110$ keV; $5/2^-$ and $3/2^-$ at 1346 and 1459 keV, respectively; and $7/2^-$, $9/2^-$ doublet at 4024 keV, are thought to be described reasonably well as a $p_{1/2}$ proton hole coupled (weakly or strongly) to the first three states of ^{20}Ne, 0^+ g.s., 2^+ at 1634 keV, and 4^+ at 4248 keV. Then, to the extent that these ^{20}Ne states can be thought as $L = 0$, 2, and 4 alpha particles coupled to an ^{16}O (g.s.) core, the ^{19}F states should be the $L = 0$, 2, and 4 alpha particles coupled to the ^{15}N (g.s.) core.

In ^{19}F, we have

$$\sigma_{\rm expt}(19,J_f) = NS_\alpha(19,J_f)\frac{2J_f+1}{2(2L+1)}\sigma_{\rm DW}(19,L) \qquad (2)$$

and in ^{20}Ne

$$\sigma_{\rm expt}(20,L) = NS_\alpha(20,L)\sigma_{\rm DW}(20,L), \qquad (3)$$

so that

$$\frac{S_\alpha(19,J_f)}{S_\alpha(20,L)} = \frac{2(2L+1)}{(2J_f+1)}\frac{\sigma_{\rm expt}(19,J_f)}{\sigma_{\rm expt}(20,L)}\frac{\sigma_{\rm DW}(20,L)}{\sigma_{\rm DW}(19,L)}, \qquad (4)$$

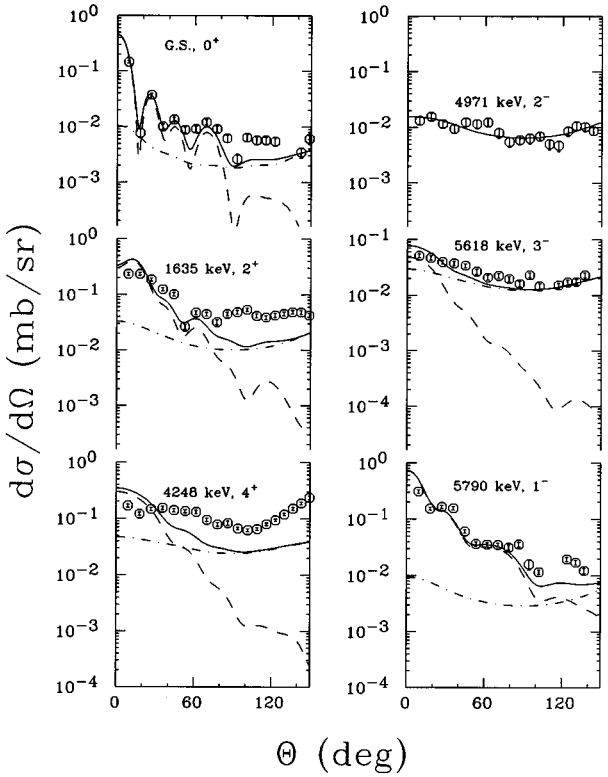

FIG. 6. Comparison of theoretical and experimental angular distributions of ^{16}O(^{6}Li,d)^{20}Ne reaction. The dot-dashed curves are HF cross sections with normalization factor of 0.61, the dashed curves are the DWBA cross sections, and the solid curves are the sum of the above two. A value of 1.94 fm for the alpha radius was used in the DWBA calculation. The normalization factors for the sum cross sections and the DWBA cross sections are the same and were obtained from the fitting of the sum cross sections to the experimental cross sections.

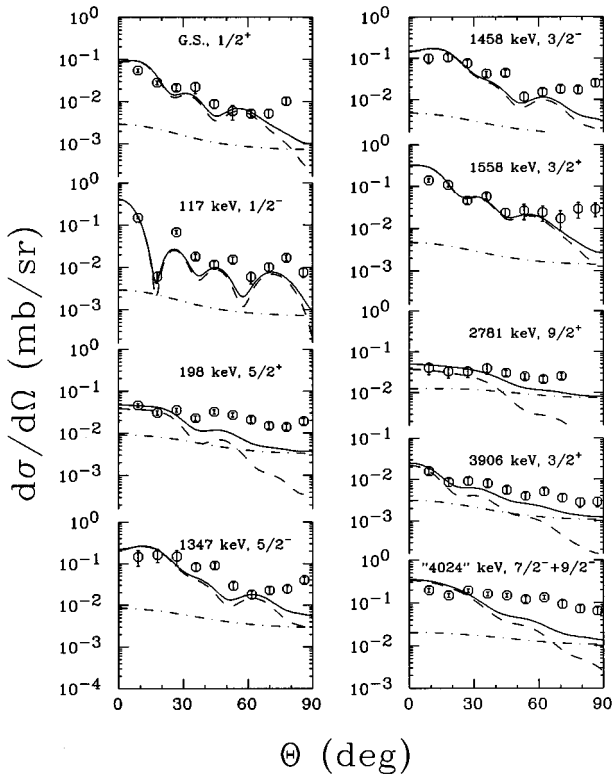

FIG. 7. Comparison of theoretical and experimental angular distributions of the ^{15}N(^{6}Li,d)^{19}F reaction. The dot-dashed curves are HF cross sections with normalization factor of 0.61, the dashed curves are the DWBA cross sections, and the solid curves are the sum of the above two. A value of 1.94 fm for the alpha radius was used in the DWBA calculation. The normalization factors for the sum cross sections and the DWBA cross sections are the same and were obtained from the fitting of the sum cross sections to the experimental cross sections.

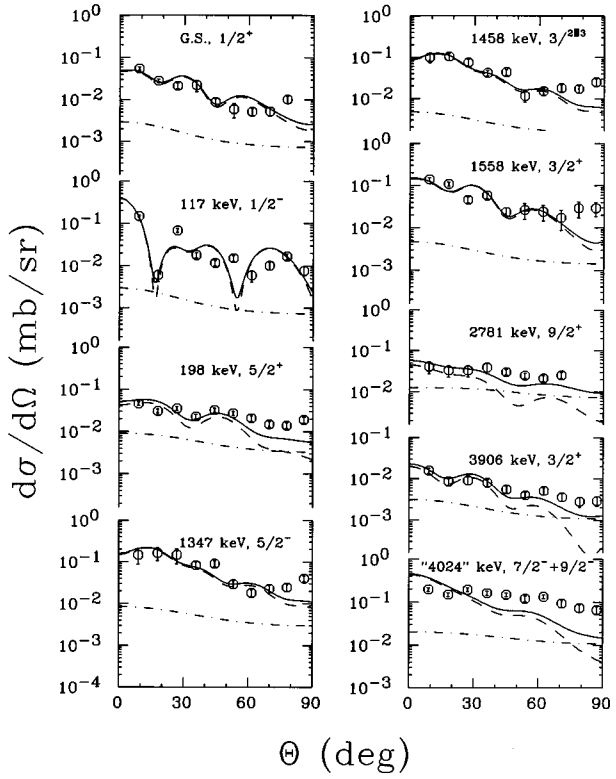

FIG. 8. Same as Fig. 7, but a value of 1.40 fm for the alpha radius was used.

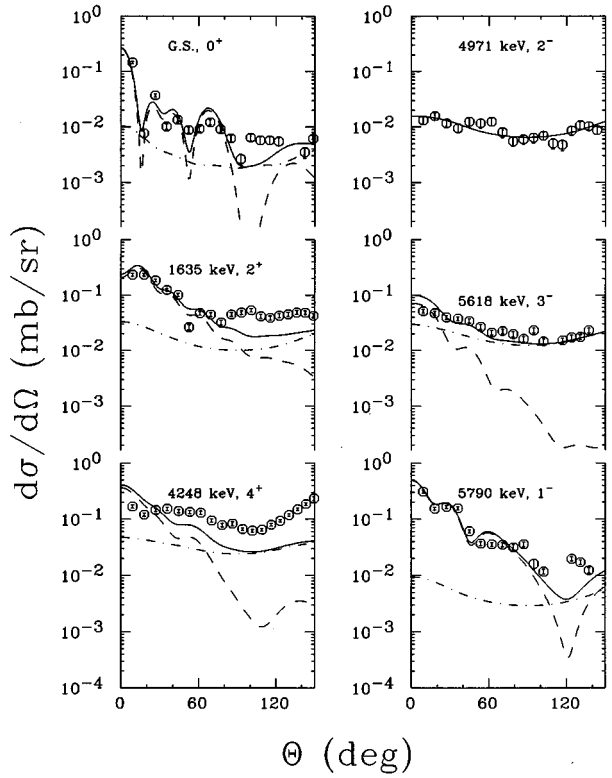

FIG. 9. Same as Fig. 6, but a value of 1.40 fm for the alpha radius was used.

where σ_{DW} is to be calculated for the appropriate A, L, and excitation energy. In ^{19}F, if we define (for $L=2$ and 4)

$$\sigma_{\mathrm{expt}}(19,L)=\sigma_{\mathrm{expt}}(19,J_f=L-\tfrac{1}{2})+\sigma_{\mathrm{expt}}(19,J_f=L+\tfrac{1}{2}), \tag{5}$$

we have

$$\frac{S_\alpha(19,L)}{S_\alpha(20,L)}=\frac{\sigma_{\mathrm{expt}}(19,L)}{\sigma_{\mathrm{expt}}(20,L)}\,\frac{\sigma_{\mathrm{DW}}(20,L)}{\sigma_{\mathrm{DW}}(19,L)}. \tag{6}$$

We display in Fig. 10, as $\times'$s, the $1/2^-$ (upper-left), summed $3/2^-$, $5/2^-$ (bottom-left), and summed $7/2^-$, $9/2^-$ (upper-right) angular distributions in ^{19}F, compared with normalized 0^+, 2^+, and 4^+ ^{20}Ne angular distributions as circles. Normalization factors are all 1.0. The corresponding σ_{DW} ratios $\sigma_{\mathrm{DW}}(20)/\sigma_{\mathrm{DW}}(19)$ are 1.1, 1.0, 0.9, respectively, when $r_{0\alpha}=1.94$ fm. While $r_{0\alpha}=1.40$ fm, they are 0.8, 0.8, and 0.7. We thus see that S_α's in ^{19}F are about the same ($r_{0\alpha}=1.94$ fm) or 80% ($r_{0\alpha}=1.40$ fm) of those in ^{20}Ne. Another consequence of the above argument is that the $5/2^-$, $3/2^-$ cross sections should be in the ratio 6:4. This is borne out by the data, as also displayed in Fig. 10 (bottom right).

The lowest $1/2^+$, $3/2^+$, $5/2^+$, and $9/2^+$ states of ^{19}F form a rotational band that is dominantly $(sd)^3$ in character. These states ideally have identical three-nucleon spectroscopic factors in ^{16}O+t [e.g., ^{16}O(^{6}Li,^{3}He)^{19}F] [10]. Coupling to the $1/2^-$ ground state of ^{15}N should produce equal alpha spectroscopic factors. We note from Table IV that this is approximately true, but only at about the 50% level.

IV. DISCUSSION

We have obtained experimental alpha spectroscopic factors for the first ten states in ^{19}F, from the ^{15}N(^{6}Li,d)^{19}F reaction at 22 MeV. In order to extract the information, the

TABLE V. Alpha spectroscopic factors of the states in ^{20}Ne.

E_x [a]	J^π [a]	S_α(DWBA)		S_α(DWBA+HF)	
0	0^+	0.14	0.97	0.13	0.95
1634	2^+	0.094	0.81	0.083	0.73
4248	4^+	0.038	0.34	0.029	0.26
4967	2^-	0	0	0	0
5621	3^-	0.0083	0.060	0.0034	0.026
5788	1^-	0.26 [b]	0.90 [b]	0.25 [b]	0.90 [b]

[a]From Ref. [7].

[b]Ratios of the alpha decay width to the alpha single-particle width calculated using ABACUS [6].

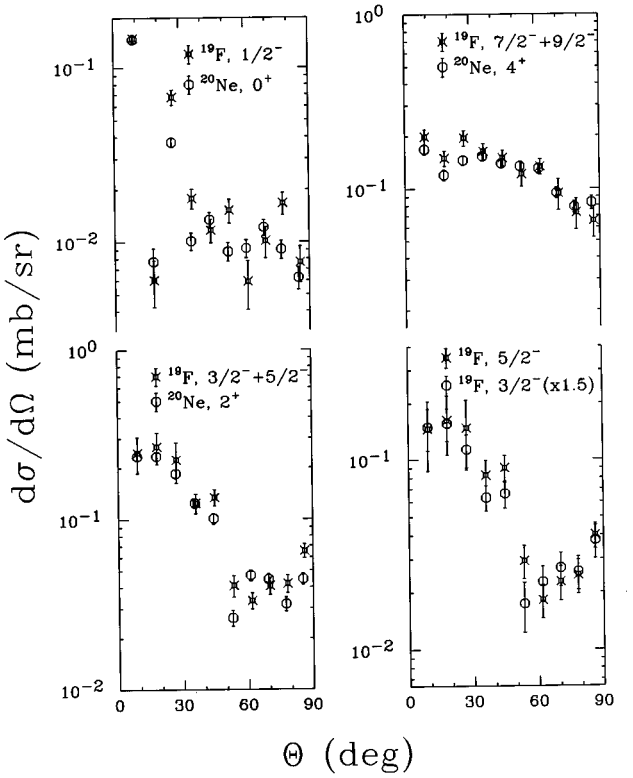

FIG. 10. Comparison of experimental angular distributions. Displayed in $\times'$s are the real experimental data. The circles present the experimental data after renormalization.

reaction ^{16}O(^{6}Li,d) has been used as a calibrator. In the calculation, we assumed the principal quanta are seven for positive-parity states and eight for negative-parity states in ^{19}F, and nine for negative-parity states, and eight for positive-parity states in ^{20} Ne. This assumption is reasonable because the ^{15}N ground state consists of mainly a p-shell hole, while the ^{16}O is a closed shell nucleus. Compound reactions contributed somewhat to the experimental cross sections. Therefore, the spectroscopic factors obtained from DWBA with HF analysis are more reliable. Uncertainties of the spectroscopic factors are smaller than 20% for the states for which the theoretical angular distributions fit the experimental data well. However, for those states for which theory cannot reproduce the experimental angular distribution shapes, the uncertainties are larger. For example, the uncertainties in the $L=4$ transfer (to the final states of $7/2^-$ and $9/2^-$ in ^{19}F and 4^+ in ^{20}Ne) are about 50%.

We have noted that both the alpha single-particle width and the DWBA cross section for α transfer feeding it are very sensitive to the value of the α potential well. This sensitivity results in quite different values of the alpha spectroscopic factor S_α for different values of $r_{0\alpha}$, but nearly identical values of alpha width $\Gamma_\alpha = S_\alpha \Gamma_{\rm sp}$. We have used the alpha width and the alpha single-particle width, calculated from the code ABACUS [6], of the 5788-keV, 1^- state in ^{20}Ne to obtain the DWBA normalization factors in our calculations. These gave us very different alpha spectroscopic factors. The spectroscopic factor computed from the experimental alpha width of ^{20}Ne (1^-) and the single-particle width using the 1.94 fm alpha radius is 0.26, while it is 0.90 from the 1.40 fm alpha radius. The alpha spectroscopic factor is from about 0.5 to 0.9 from the previous measurements of ^{16}O(^{6}Li,d) [2,14] and ^{16}O(^{7}Li,t) [18,15,16]. Furthermore, as noted above, according to the weak-coupling model, the $K^\pi = 1/2^-$ band in ^{19}F has $(sd)^4$ structure coupled to a $p_{1/2}$ hole [17]. In the (^{7}Li,t) reaction on ^{15}N and ^{16}O, an enhancement of the cross section in the ^{15}N(^{7}Li,t)^{19}F transitions by a factor of about 2 over that in the ^{16}O(^{7}Li,t)^{20}Ne transitions was observed [18]. It indicates that the negative-parity states in ^{19}F could perhaps have larger alpha spectroscopic factors. In the present measurement of ^{15}N(^{6}Li,d), the reaction populated negative-parity states more strongly than than positive-parity states (for details, see Table I).

We calculated the alpha-particle width for the 4033-keV, $3/2^+$ state in ^{19}Ne, and obtained values of 11 μeV with $r_{0\alpha}=1.40$ fm and 12 μeV with $r_{0\alpha}=1.94$ fm. These values are only about 10% larger than those the authors obtained in an almost parameter free method [19]. Uncertainties for each of those values contain contributions of 10% from the measured direct component of the cross section, an estimated 4% from the ratios of $\sigma_{\rm DW}$, and 11% from the experimental value of Γ_α for ^{20}Ne (1^-). There is about 30% difference between the values for $r_{0\alpha}=1.40$ and 1.94 fm. With $r_{0\alpha}=1.40$ fm, Γ_α is 8.8 μeV for $q=9$ and 11.0 μeV for $q=7$. The average is 9.9 ± 1.5 μeV. With $r_{0\alpha}=1.94$ fm, the spread in Γ_α is only slightly larger and the average is 13.2 ± 2.0 μeV. Therefore, though only relative spectroscopic factors can be obtained from DWBA, absolute particle widths can be extracted from the analysis. Using these alpha widths, we obtained about the same reaction rates for the ^{15}O(α,γ)^{19}Ne at the temperatures of astrophysical interest. The new rates are about 50% to 100% larger than that used by Langanke *et al.* [20] and Magnus *et al.* [21].

The authors thank D. Koltenuk for assistance with the calculations. This work was supported by the National Science Foundation.

[1] D. W. Heikkinen and W. Feldman, Nucl. Phys. **A113**, 57 (1968).
[2] N. Anantaraman, H. E. Gove, R. A. Lindgrem, J. Tōke, J. P. Trentelman, J. P. Draayer, F. C. Jundt, and G. Guillaume, Nucl. Phys. **A313**, 445 (1979).
[3] L. J. House and K. W. Kemper, Phys. Rev. C **17**, 79 (1978).
[4] G. D. Gunn, R. N. Bord, N. Anantaraman, D. Shapira, J. Toke, and H. E. Jone, Nucl. Phys. **A275**, 524 (1977).
[5] A. E. Champagne and M. Wiescher, Annu. Rev. Nucl. Part. Sci. **42**, 39 (1992).
[6] S. Zawadski, ABACUS computer code, Argonne National Laboratory, 1962 (unpublished).
[7] F. Ajzenberg-Selove, Nucl. Phys. **A475**, 1 (1987).
[8] J. W. Watson, Nucl. Phys. **A198**, 129(1972).

[9] U. Strohbusch, W. Schmidt, and G. Huber, Nucl. Phys. **A163**, 453 (1971).
[10] J. D. Garrett, H. G. Bingham, H. T. Fortune, and R. Middleton, Phys. Rev. C **5**, 682 (1972).
[11] H. T. Fortune, M. N. I. Al-Jadir, R. R. Betts, J. N. Bishop, and R. Middleton, Phys. Rev. C **19**, 756 (1979).
[12] P. D. Kunz, DWUCK4 computer code, University of Colorado, 1981 (unpublished).
[13] R. Stokstad, STATIS computer code, Brook Haven National Laboratory, 1992 (unpublished).
[14] T. Tanabe, M. Yasue, K. Sato, K. Ogino, Y. Kadota, Y. Taniguchi, K. Makino, and M. Tochi, Phys. Rev. C **24**, 2556 (1981).
[15] H. S. Bradlow, W. D. M. Rae, P. S. Fisher, N. S. Godwin, G. Proudfoot, and D. Sinclair, Nucl. Phys. A **314**, 171 (1979).
[16] S. G. Cooper, J. Phys. G **12**, 371 (1986).
[17] S. Mordechai and H. T. Fortune, Phys. Rev. C **29**, 1765 (1984).
[18] K. I. Kubo, F. Nemoto, and H. Bando, Nucl. Phys. A **224**, 573 (1974).
[19] Z. Q. Mao, H. T. Fortune, and A. G. Lacaze, Phys. Rev. Lett. **74**, 3760 (1995).
[20] K. Langanke, M. Wiescher, W. A. Fowler, and J. Görres, Astrophys. J. **301**, 629 (1986).
[21] P. V. Magnus, M. S. Smith, A. J. Howard, P. D. Parker, and A. E. Champagne, Nucl. Phys. **A506**, 332 (1990).